Survival impact of [225Ac]Ac-DOTATOC alpha-therapy in a preclinical model of pancreatic neuroendocrine tumor liver micrometastases

Alexandre Lugat, Nicolas Chouin, Florian Chocteau, Mathilde Esnault, Séverine Marionneau-Lambot, Sébastien Gouard, Éric Frampas, Alain Faivre-Chauvet, Mickaël Bourgeois, Alfred Morgenstern, et al.

Title page

Survival impact of [^{225}Ac]Ac-DOTATOC alpha-therapy in a preclinical model of pancreatic neuroendocrine tumor liver micrometastases.

Authors:
Alexandre Lugat [1,2,3], Nicolas Chouin [3], Florian Chocteau [3], Mathilde Esnault [3], Séverine Marionneau-Lambot [3], Sébastien Gouard [3], Éric Frampas [3,4], Alain Faivre-Chauvet [2,3], Mickaël Bourgeois [2,3], Alfred Morgenstern [5], Frank Bruchertseifer [5], Michel Chérel [3,6], Françoise Kraeber-Bodéré [2,3#], Catherine Ansquer [2,3#] and Joëlle Gaschet [3#*]

1. Medical Oncology Department, Nantes University Hospital, 44000 Nantes, France.
2. Nuclear Medicine Department, University Hospital, Nantes, France.
3. Nantes-Angers Cancer Research Center CRCI2NA, University of Nantes, INSERM UMR1307, CNRS-ERL6075, Nantes, France.
4. Central Department of Radiology and Medical Imaging, Nantes University Hospital, 44000 Nantes, France.
5. European Commission, Joint Research Centre, Directorate for Nuclear Safety and Security, Karlsruhe, Germany.
6. Department of Nuclear Medicine, Institut de Cancérologie de l'Ouest (ICO) - Site Gauducheau, Saint-Herblain, France.

[#] Last Authors contributed equally to this work

Alexandre Lugat, MD, PhD, service de médecine nucléaire, Centre hospitalier universitaire de Nantes, 1, place Alexis Ricordeau, 44000 Nantes.
tel : +33240084136
Fax : +33240084218
alexandre.lugat@chu-nantes.fr

* Corresponding author:
Joëlle Gaschet, PhD, Institut de Recherche en Santé de l'Université de Nantes, CRCI2NA – INSERM UMR1307, CNRS-ERL6075, 8 quai Moncousu, BP70721, 44007 Nantes cedex 1, France.
joelle.gaschet@univ-nantes.fr

Word count: 6312 words.

Short title: [^{225}Ac]Ac-DOTATOC to treat metastatic NET.

Funding:
This work has been supported in part by grants from the French National Agency for Research "France 2030 investment plan" Labex IRON (ANR-11-LABX-18-01) and RHU OPERANDI (ANR-21-RHUS-0012) and by grant from INCa-DGOS-INSERM/ITMO Cancer_18011 (SIRIC ILIAD) and by grant from "Fondation pour la Recherche Médicale" (FRM FDM202006011156).

Abstract

Although peptide radionuclide therapy (PRRT) using a somatostatin analog (SSA) radiolabeled with a beta-emitter: [^{177}Lu]Lu-DOTATATE has shown a good clinical efficacy in neuroendocrine tumors (NETs), most of the patients only achieved tumoral stabilization and rare but severe long-term hematological toxicities have been reported. One of the promising options to improve PRRT is targeted alpha therapy. It is therefore essential to propose animal models that can mimic systemic spread disease, especially microscopic disease such as early stage of NET liver metastases to explore targeted alpha therapy. Herein, we report the evaluation of efficacy and toxicity of [^{225}Ac]Ac-DOTATOC in an original preclinical murine model simulating the development of well-characterized liver metastases of pancreatic NETs with SSTR overexpression. **Methods**: A mouse model of liver metastases of pancreatic NETs was developed by intraportal injection of AR42J cells and explored using [^{68}Ga]Ga-DOTATOC and [^{18}F]F-FDG PET/MRI. Biodistribution study and radiation dosimetry of [^{225}Ac]Ac-DOTATOC were determined in subcutaneous tumor-bearing NMRI-nude mice. Efficacy and toxicity were determined by intravenous injection of increasing activities of [^{225}Ac]Ac-DOTATOC 10 days after intraportal graft. **Results**: Liver tumors showed a high uptake of [^{68}Ga]Ga-DOTATOC and no uptake of [^{18}F]F-FDG confirming the well-differentiated phenotype. All groups treated with [^{225}Ac]Ac-DOTATOC showed a significant increase in overall survival compared with DOTATOC-treated mice, especially those treated with the highest activities: 53 days with 240 kBq ($p=0.0001$), and 58 days with 2x120 kBq ($p<0.0001$) vs 28 days with non-radiolabeled DOTATOC. On blood tests, a transient and moderate decreased in white blood cells count after treatment and no severe hepatic or renal toxicity were observed after treatment which was consistent with pathological and radiation dosimetry findings. **Conclusion**: [^{225}Ac]Ac-DOTATOC exhibit a favorable efficacy and toxicity profile in a mouse model of liver micrometastatic pancreatic NET.

Keywords: Neuroendocrine tumor, targeted alpha therapy, PET/MRI, actinium-225, somatostatin analogs.

Text

Introduction

Neuroendocrine tumors (NETs) are a heterogenous group of tumors arising from the diffuse neuroendocrine system. Gastro-enteropancreatic (GEP-NETs) are the most common primary tumor site with an increasing incidence [1]. The overexpression of somatostatin receptors (SSTR), especially subtype 2 [2,3] has led to the development of a phenotypical specific whole-body imaging using somatostatin analogs (SSA) [4]: monophotonic scintigraphy using ^{111}Indiethylenetriamine-pentaacetic acid-octreotide (Octreoscan®) [5] then hybrid positron emission tomography (PET) and computed tomography (CT) using ^{68}Ga-labeled SSA with better performances [6,7].

At metastatic stage, GEP-NETs management range from wait and watch strategy to systemic treatment [8]. In the last years, treatment of GEP-NETs has improved with the development of peptide receptor radionuclide therapy (PRRT). Indeed, based on the same concept of tumor SSTR overexpression, therapy with SSA radiolabeled with beta-emitters has emerged. The NETTER-1 trial published in 2017 has established PRRT with [^{177}Lu]Lu-DOTATATE as a second line option for progressive midgut NETs in case of sufficient SSTR expression which has led to FDA and EMA approvals in 2018 [8,9]. Although PRRT with beta-emitters has been demonstrating good clinical efficacy and improved quality of life, most of the patients only achieved tumoral stabilization with [^{177}Lu]Lu-DOTATATE. Indeed, overall tumor response rates range from 6% to 33% of patients. For example, in the NETTER-1 study, out of 111 patients treated with [^{177}Lu]Lu-DOTATATE only one achieved a complete response and 14 showed a partial response [9]. Furthermore, within two to three years, disease progression occurs in approximately half of the patients, necessitating additional lines of treatment [9–11]. Additionally, PRRT with [^{177}Lu]Lu-DOTATATE is generally well tolerated but severe long-term hematological toxicity such as myelodysplastic syndrome and leukemia have been reported in close to 3% of the patients [12,13].

These results may be attributed to the characteristics of beta-particles, which are low linear-energy transfer (LET) particles (0.2 keV/µm), with a relatively long path through the tissue (1-10mm). Tumor cell death primarily occurs through DNA single strand breaks while DNA double strand breaks and ionization are less frequent [14]. Furthermore, healthy cells surrounding the targeted tumor cells are also exposed to radiation, which can contribute to toxicity [15]. For all these key reasons, there is a need to develop new radiopharmaceuticals capable of improving overall survival and tumor response.

Alpha-particles, composed of two neutrons and two protons, have a greater mass and a double-positive charge, along with a high energy range of 4 to 10 MeV, in contrast to beta-particles. This increased mass and charge result in limited tissue penetration (50-100 µm) and a higher linear energy transfer (LET) of 50-230 keV/µm, inducing complex and irreparable DNA double-strand breaks. Alpha-particles deposit significantly more energy along their path compared to beta-particles. These characteristics account for their strong cytotoxic effects, while sparing surrounding healthy tissues [14,16].

One promising alpha-emitter is ^{225}Ac which has a half-life of nearly 10-days and a long decay scheme that generates four alpha-particles contributing to a potential high tumor cytotoxicity [17]. Tumor responses have been reported using compassionate injections of ^{225}Ac-labeled SSA in patients with metastatic NET in progression after PRRT with beta-emitters [18,19] and two studies in animal models of subcutaneous tumors have further shown promising results. First, Miederer *et al*. found that, in a model of pancreatic NET that 12 to 20kBq [^{225}Ac]Ac-DOTATOC reduced tumor growth with improved efficacy compared to [^{177}Lu]Lu-DOTATOC, as well as lower toxicity. Nonetheless, mice injected with activities above 30kBq developed chronic nephropathy [20]. The efficacy of [^{225}Ac]Ac-DOTATATE was also reported in another subcutaneous model of carcinoid lung tumor overexpressing SST2, albeit with different toxicity profile and in particular no renal pathological changes up to 111kBq.[21].

However, based on their physical properties, the optimal setting for alpha-particles therapy is probably the stage of micrometastases, early relapse, or the stage of minimal disease observed after surgical treatment or induction therapy in an attempt to eradicate residual tumor cells. But this context of treating patients earlier, with potentially longer survival implies acceptable and limited toxicity. New preclinical models are therefore essential, and the subcutaneous tumor-graft mouse models proposed to date, while convenient, are not the most relevant to evaluate alpha-particles therapy of NETs at these stages of the disease. Indeed, despite their initially slow progression, a notable proportion of NETs advance to later stages. Among these, liver involvement stands out as the most frequent occurrence, significantly compromising patient prognosis [22,23]. It is therefore essential to propose animal models that can mimic systemic spread disease, especially microscopic disease such as early stage of NET liver metastases.

The aim of the present study was thus to evaluate efficacy and toxicity of [^{225}Ac]Ac-DOTATOC in an original preclinical murine model simulating the development of well-characterized liver metastases of pancreatic NETs with SSTR overexpression.

Materials and methods

Cell line

AR42J is a rat pancreatic amphicrine cell line derived form an acinar cell carcinoma provided by American Type Culture Collection (ATCC ®), Manassas, VA (lot 63848927) which strongly express SSTR2, chromogranin A and synaptophysin. Cells were grown in Dulbecco's Modified Eagle Medium (DMEM, Gibco®) supplemented with 20% heat-inactivated fetal calf serum (PAA Laboratories®), 2mM L-glutamine (Gibco®), penicillin (1000 u/mL) and streptomycin (1mg/mL) (Gibco®). They were maintained at 37°C in a 5% CO_2 humidified air atmosphere.

Animals

All animal experiments were carried out in accordance with the European directive 2010/63/EU on the protection of laboratory animals and its transposition into French law (decree n 2013-118) and were conducted on the Experimental Therapeutic Unit platform (SFR François Bonamy, IRS-UN, University of Nantes, license number: D44-278). The study was approved by the Ethics Committee of French Ministry of Higher Education and Research (protocol no. APAFIS#22777). Female NMRI-nude (nu/nu) mice aged 8 to 12 weeks old (Janvier®, Le Genest St Ile, France) were housed under standard condition in ventilated cages (5 mice per cage) under sterile and pathogen-free conditions with free access to food and water *ad libitum.* All animal experiments, whether subcutaneous or intraportal grafts, were performed with AR42J cells that had undergone 13 passages or fewer. To confirm *in vivo* phenotype stability preliminary histopathological studies on hepatic tumors to confirm SSTR2 expression have been performed. Methods and results are available in the **Supplementary Information**.

Intraportal tumor graft procedure

Twenty minutes before the procedure starts, mice received a standard dose of 0.1mg/kg (50µL) buprenorphine subcutaneously. They were anesthetized by an intra-peritoneal injection of a ketamine and xylazine hydrochloride mixture (100 mg/kg Ketalar® ketamine, 10 mg/kg 2% Rompun®, CentraVet France) at a volume of 100µL per 10g of mouse. Anesthesia was checked by pinching the hind paw. Corneal protection was applied (Ocrygel, CentraVet, France).

After a short laparotomy, $1x10^6$ AR42J cells suspended in 100µL Phosphate-Buffered Saline (PBS) solution were injected into the portal vein through a 29G needle as described by Frampas et al [24]. As post-operative pain after laparotomy was judged “severe”, analgesia included 15µg/kg (50µL) buprenorphine subcutaneously

for 3 days combined with 5 days of non-steroidal anti-inflammatory drugs in drinking water (meloxicam 2mg/kg/d, Metacam®, Boehringer Ingelheim France).

Post-operative monitoring was performed daily, and animals were sacrificed in case of marked distress signs, a weight loss greater than 20% of initial body weight, icterus, or ascites.

MRI and PET/MRI imaging

Mice were anesthetized 5 min prior to acquisition with 5% isoflurane using oxygen as a carrier then placed on a heated sled and kept sedated with 3 to 4% isoflurane with a suitable mask during the imaging experiment.

Magnetic resonance imaging (MRI), hybrid positron emission tomography (PET) and magnetic resonance imaging (PET/MRI) studies were performed with a 3.0 T system provided by RS2D with a HALO 3.0 PET insert provided by Inviscan at the Center for Applied Multimodal Imaging (CIMA, Nantes, France).

The following sequences were used for all MRI sessions: 3D T1-weigted coronal rapid acquisition with relaxation enhancement (RARE) (TE = 12.06ms, TR = 769ms, 80x40x31 mm FOV, 5 averages, 31 slices, 0.8mm thickness with 0.2ms gap between slices, 450x144x31 matrix), 3D T2-weigted coronal RARE (TE = 64.49ms, TR = 5000ms, 78x32x27.9mm FOV, 6 averages, 31 slices, 0.8mm thickness with 0.1ms gap between slices, 450x144x31 matrix) with and without fat-saturation.

The HALO 3.0 PET spatial resolution was 1.0mm, the field of view was 40mm axial. The PET images 3D T1 weighted RARE images were simultaneously acquired and were reconstructed with the 3D-OSEM algorithm (3-dimensional ordered-subsets expectation maximization algorithm).

PET and MRI images were converted into DICOM format and processed with OsiriX Medical Imaging software (version 11.0.1, Pixmeo, Bernex, Switzerland).

Concerning phenotypical imaging studies, 5 mice were injected intravenously with 5 MBq [^{68}Ga]Ga-DOTATOC and imaged by PET/MRI 1 hour after the injection This study was performed at day 23 to be sure to visualize macro-tumors in the liver to characterize their phenotype. The same mice, at day 25, were fasted for 4 hours then injected intravenously with 4 MBq [^{18}F]F-FDG and imaged one hour later. DOTATOC radiolabeling with ^{68}Ga is described in the **Supplementary Information.**

[^{225}Ac]-DOTATOC alpha-therapy

DOTATOC radiolabeling with ^{225}Ac, ex-vivo biodistribution and dosimetry are described in the **Supplemental Information.**

A preliminary dose-limiting study was performed using a single i.v. injection of [^{225}Ac]Ac-DOTATOC at 20kBq (n=3), 40kBq (n=3), 80kBq (n=4), 120kBq (n=3) and 180kBq (n=4) in non-grafted female NMR-nude (nu/nu) mice.

On the evidence of these results **(Supplemental Fig. 3, 4),** an efficacy study was then carried using [^{225}Ac]Ac-DOTATOC with a single i.v. injection of 120kBq (n=9), 180kBq (n=9), 240 kBq (n=11) at Day 10 after intraportal tumor graft (microscopic disease) or as two i.v. injections of 120kBq (n=11) at Day 10 and Day 23 after graft. The control group have received i.v. injection of non-radiolabeled DOTATOC (n=10). Finally, the total mass of DOTATOC (5.3 µg) injected into each mouse was identical, the mixtures being adjusted with unlabeled peptide when necessary.

Animals were monitored every two to three days. Tumoral volumes were assessed by MRI every week and before sacrifice and delineated using OsiriX Medical Imaging software (version 11.0.1, Pixmeo, Bernex, Switzerland).

Hematological, kidney and liver toxicities were assessed at Day 10, 21, 35, 49 after therapy in all treated mice. In the control group blood sample were collected at Day 10, 21 and 29. Blood samples were collected from the retroorbital sinus in EDTA tubes (15µL for hematological analysis) and Lithium-Heparin tubes (100µL for biochemical analysis) after a local anesthesia with 1% tetracaine. Hematological parameters were determined using an automated quantitative analyzer (Element HT5, scil Animal Care, Altorf, France) and biochemical parameters using an automatic biochemistry analyzer (Element RC, scil Animal Care, Altorf, France). Liver toxicity was determined by measurement of alkaline phosphatase (ALP), alanine aminotransferase (ALT) and total bilirubin (TBIL). Kidney toxicity was determined by measurement of blood urea nitrogen (BUN) and creatinine.

Endpoints were weight loss ≥ 20% of initial body weight, marked distress signs, lethargy, total tumoral liver ≥ 1000mm^3 as evaluated by MRI, ascites, icterus, or digestive hemorrhage.

Kidney anatomopathological analysis

Both kidneys were collected from 10 control and 15 treated mice (5 in the 240 kBq group and 10 in the 120x2 kBq group). Three-micrometers-thick tissue sections of formalin-fixed, paraffin-embedded (FFPE) bilateral kidneys were stained with hematoxylin–eosin-saffron (HES) and adjudicated under light microscopy by a veterinary pathologist. Semiquantitative scores of kidney lesions (0 to 5 points for no lesion to severe and diffuse

lesion) was established thanks to the classification INHAND (International Harmonization of Nomenclature and Diagnostic Criteria for Lesions in Rats and Mice) [25].

Statistical analysis

Statistical analyses were performed using Prism 9.3.0 (GraphPad Software, Inc., San Diego, CA, USA). All data are presented as median or mean ± standard deviation. Survival curves were compared using a log-rank (Mantel–Cox) test. For toxicity analysis, a two-factor ANOVA followed by a Sidak's multiple comparison test was performed.

Results

Animal model development

A first group of 15 mice was grafted by intraportal injection of $1x10^6$ AR42J tumor cells to investigate the development of the disease without any treatment. After the surgery, mice lost weight, but never more than 10% of their initial body weight. Mice regained their initial weight in 7.7 ± 2.9 days on average (**Supplemental Fig. 4, A**). By Day 12, all mice had recovered their initial weight or more.

MRI allowed to follow the development of the tumors in the liver over the period leading up to the death of the animals (**Fig. 1**). Liver tumors appeared hyperintense in T2-weighted sequences and hypointense in T1-weighted sequences. The first liver tumors appeared as early as Day 15 and we could detect liver tumors as small as 0.8 mm, confirmed by follow-up. The median detection time of the first tumor by MRI was 20 days and the median overall survival without any treatment was 28 days (**Supplemental Fig. 4, B, C**). Mice were sacrificed mainly because of weight loss (n=4), jaundice (n=8) or digestive occlusion (n=3).

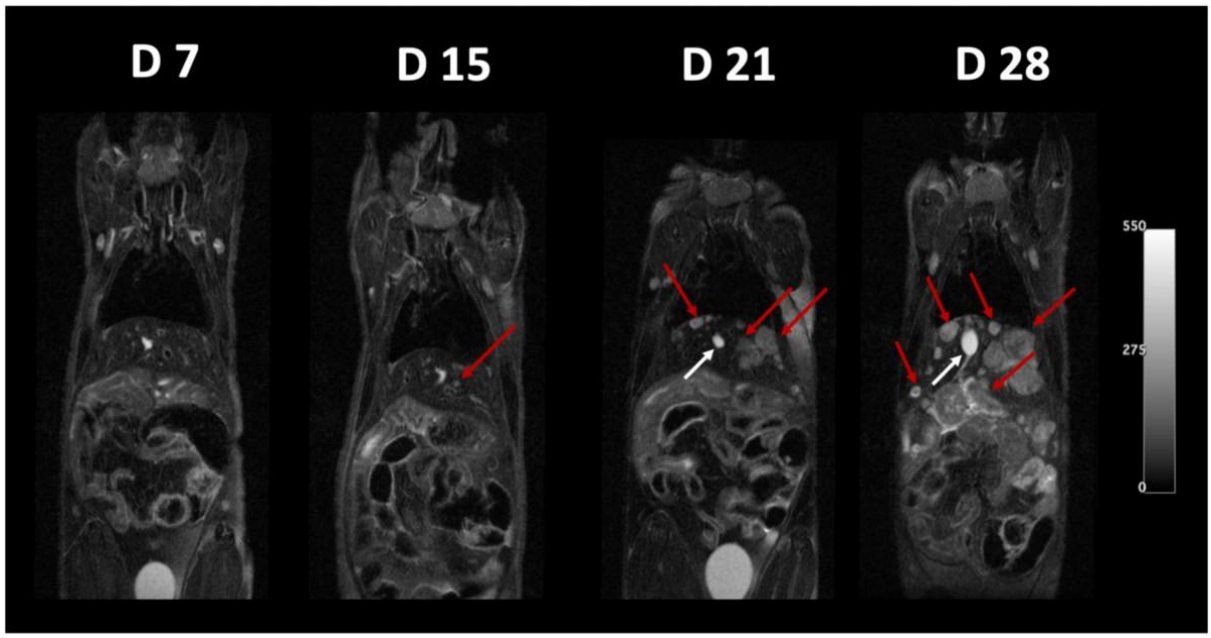

Fig. 1 *MRI follow-up of the same mice over-time (T2-weigted coronal RARE with fat saturation). Day 7, 15, 21 and 28. Red arrows: liver tumors. White arrows: gallbladder.*

Characterization of tumor phenotype

[^{68}Ga]Ga-DOTATOC and [^{18}F]F-FDG PET/MR were successively performed in a group of 5 mice (**Fig. 2, A, B, C).** On the [^{18}F]F-FDG-PET/MRI images, no uptake was observed in liver tumors whereas these tumors exhibited high uptake of [^{68}Ga]Ga-DOTATOC. Every tumor detected by MRI showed a high uptake of [^{68}Ga]Ga-DOTATOC, with the exception of one mouse that had a single tumor with a longest axis of 1.1 mm. All other tumors were > 2.0 mm or confluent.

These results confirmed the well-differentiated phenotype *in vivo*, with overexpression of SSTR and a relatively slow glucose metabolism. These data are also consistent with [^{68}Ga]Ga-DOTATOC and [^{18}F]F-FDG biodistribution at 1h p.i. (**Supplemental Fig. 5 and Supplemental Table 1**).

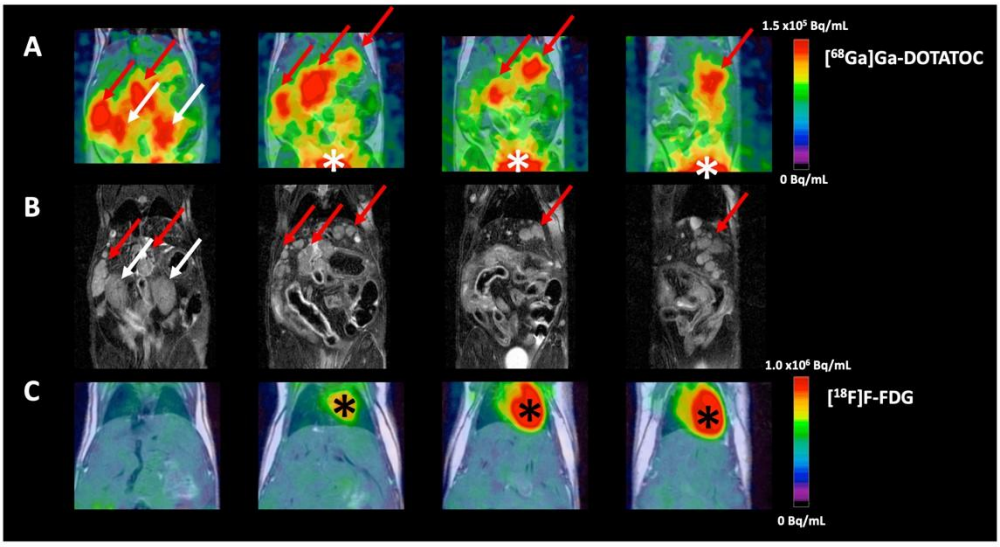

***Fig. 2** Multiple slices of the same mice explored with A. [^{68}Ga]Ga-DOTATOC PET/RMI at Day 23, B. MRI T2 weighted coronal RARE with fat saturation at day 23 and C. [^{18}F]F-FDG PET/MRI at Day 25. Red arrows: liver tumors, white arrows: kidneys, white asterisks: bladder. Black asterisk: heart.*

Ex vivo biodistribution of [^{225}Ac]-DOTATOC

Ex vivo biodistribution study was performed on a group of 24 subcutaneous AR42J tumor-grafted mice and macroscopic tumors were obtained in 19 of them.

[^{225}Ac]Ac-DOTATOC showed favorable tumor uptake with 5.91 ± 0.99 % IA/g as early as 5 min p.i. which was then relatively stable between 1h and 24h. Rapid blood clearance of radiolabeled peptide was observed, with blood activity concentration rapidly decreasing from 6.34 ± 0.48 % IA/g at 5 min p.i. to 0.49 ± 0.15 at 1h p.i. As a SSA, [^{225}Ac]Ac-DOTATOC displayed high accumulation in the kidney with 22.84 ± 3.19 % IA/g at 5 min p.i. but rapidly decreased to 5.47 ± 0.79 % IA/g at 4h p.i. (**Fig. 3, A**). At 24h, tumor uptake and kidney uptake were

similar with 3.31 ± 0.69 % IA/g in the tumor compared with 3.19 ± 0.69 % IA/g in the kidney. Very low uptake was observed in other organs, < 1 % IA/g as early as 1h p.i..

Finally, the tumor to tissue ratio was rapidly favorable (>1) in all organs as early as 1h p.i., particularly in the liver (5.6 ± 0.25 at 1h p.i.) with the exception of the kidney, where the ratio was > 1 at 24h (**Fig. 3, B).** Complete biodistribution data are presented in **Supplemental Table 2**.

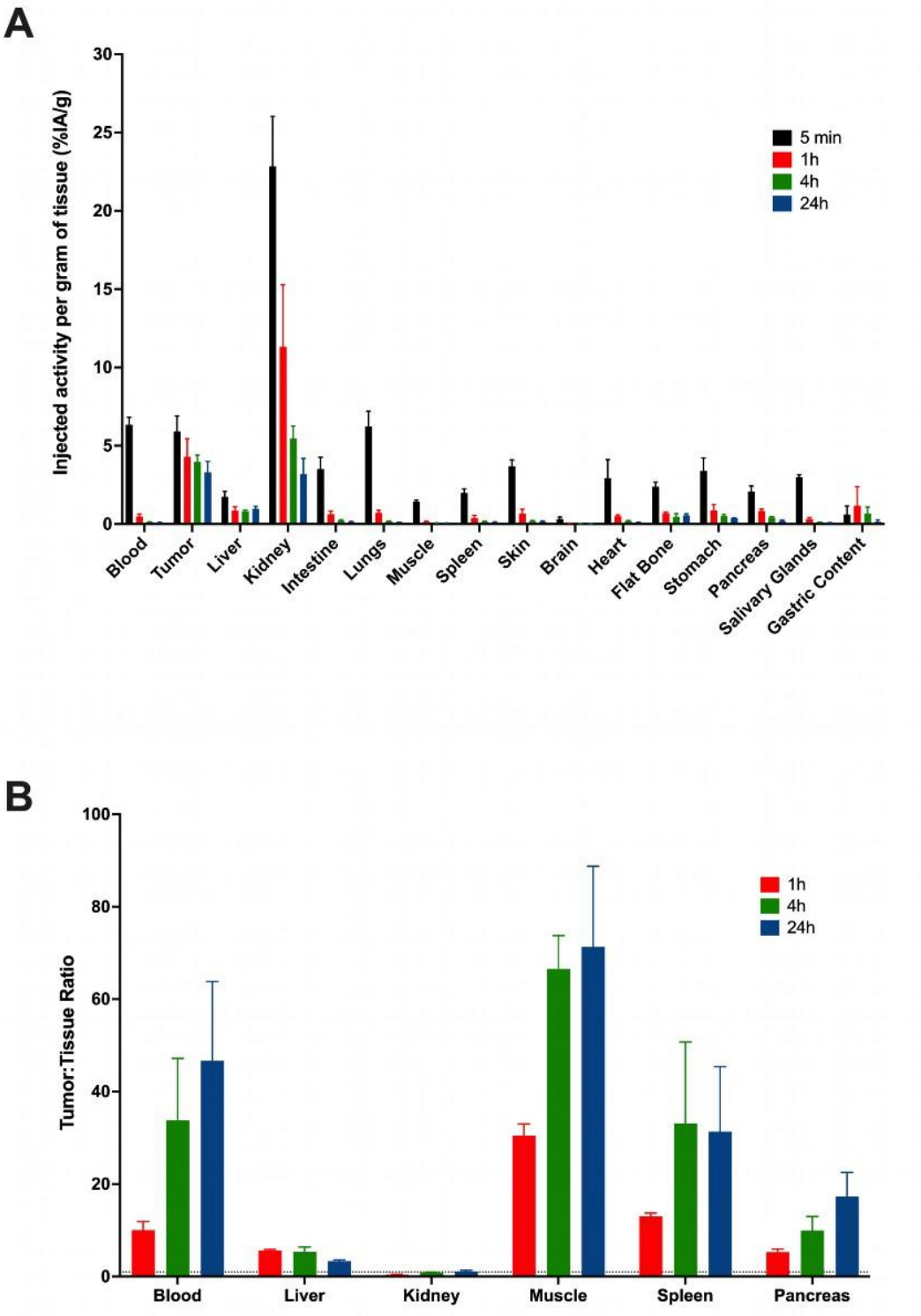

286
287

288 ***Fig. 3*** *A. Ex vivo biodistribution of [^{225}Ac]Ac-DOTATOC in AR42J tumor-grafted mice at 5min, 1, 4 and 24h. Values are*
289 *expressed as %IA/g ± SD. B. Tumor:tissue ratio for selected organs at 1, 4 and 24h. Dotted line=1.*

290

Dosimetry

Dosimetry calculations for single injection of [^{225}Ac]Ac-DOTATOC were performed based on *ex vivo* biodistribution. The mean absorbed dose per MBq or for a single injection of the highest activity studies (240kBq) are available in **Table 1**.

Table 1: Estimated absorbed doses to tissue/organs per MBq or for a single injection of [^{225}Ac]Ac-DOTATOC in AR42J tumor-grafted mice.

Organ/Tissue	Mean absorbed dose ± SD (Gy/MBq)	Mean absorbed dose ± SD (Gy) for 240 kBq
Blood	0.5 ± 0.1	0.1 ± 0.0
Tumor	67.4 ± 4.7	16.2 ± 1.1
Liver	51.7 ± 9.6	12.4 ± 2.3
Kidneys	50.3 ± 4.7	12.1 ± 1.1
Intestine	2.3 ± 0.2	0.6 ± 0.1
Lungs	3.2 ± 0.3	0.8 ± 0.1
Muscle	0.1 ± 0.0	0.0 ± 0.0
Spleen	4.5 ± 1.2	1.1 ± 0.3
Skin	3.3 ± 0.3	0.8 ± 0.1
Brain	0.6 ± 0.2	0.2 ± 0.1
Heart	2.7 ± 0.5	0.7 ± 0.1
Flat bone	32.7 ± 9.5	7.8 ± 2.3
Stomach	10.3 ± 1.1	2.5 ± 0.3
Pancreas	4.3 ± 0.4	1.0 ± 0.1
Salivary glands	2.1 ± 0.3	0.5 ± 0.1

The tumor received the highest absorbed dose with 67.4 ± 4.7 Gy/MBq followed by the liver and kidneys with 51.7 ± 9.6 Gy/MBq and 50.3 ± 4.7 Gy/MBq. With a single 240kBq injection, the mean absorbed dose to the kidneys did not exceed 23 Gy. Tumor-to-tissue absorbed dose ratios were favorable in all organs (>1), especially in the kidneys and liver with 1.3.

Efficacy of [^{225}Ac]Ac-DOTATOC in pancreatic neuroendocrine tumor liver micrometastases mice.

Median time to detection of the first tumor by MRI in animals treated with non-radiolabeled DOTATOC was 21 days with an overall survival of 28 days, which was similar to previous non-treated control mice.

Compared with DOTATOC-treated mice, all groups of mice treated with [^{225}Ac]Ac-DOTATOC showed a significant increase in overall survival: 53 days with 240kBq ($p=0.0001$), 58 days with 2x120kBq ($p<0.0001$), 43 days with 180kBq ($p=0.015$) and 43 days with 120kBq ($p=0.0012$) (**Fig. 4, A**). In terms of time to first tumor detection on MRI, apart from the 120kBq group, all other groups showed a significant increased median time: 42 days with 240kBq ($p=0.0027$), 49 days with 2x120kBq ($p=0.0004$), and 35 days with 180kBq ($p=0.0042$) (**Fig. 4, B**).

Interestingly, the two groups treated with the same cumulated activity of 240kBq (single i.v. injection of 240kBq at Day 10 or two i.v. injections of 120kBq: one at Day 10 and one at Day 23) were not different in terms of overall survival (53 days and 58 days respectively, $p=0.45$) or in time to detection of the first tumor by MRI (42 days and 49 days respectively, $p=0.16$). However, when compared with lower activity group, mice treated with two i.v. injections of 120kBq were the group with the best efficacy as it showed a significant increased overall survival compared to 120kBq and 180kBq ($p=0.0005$ and $p=0.024$, respectively) as well as a significant longer time to first tumor detection on MRI ($p=0.0001$ and $p=0.006$, respectively). Indeed, although mice treated with one injection of 240kBq showed a significantly increased overall survival compared to 120kBq ($p= 0.0041$) and a significantly longer time to detection of the first tumor on MRI ($p=0.0041$) this was not the case compared to the 180kBq group (overall survival $p=0.17$ and detection of the first tumor $p=0.077$).

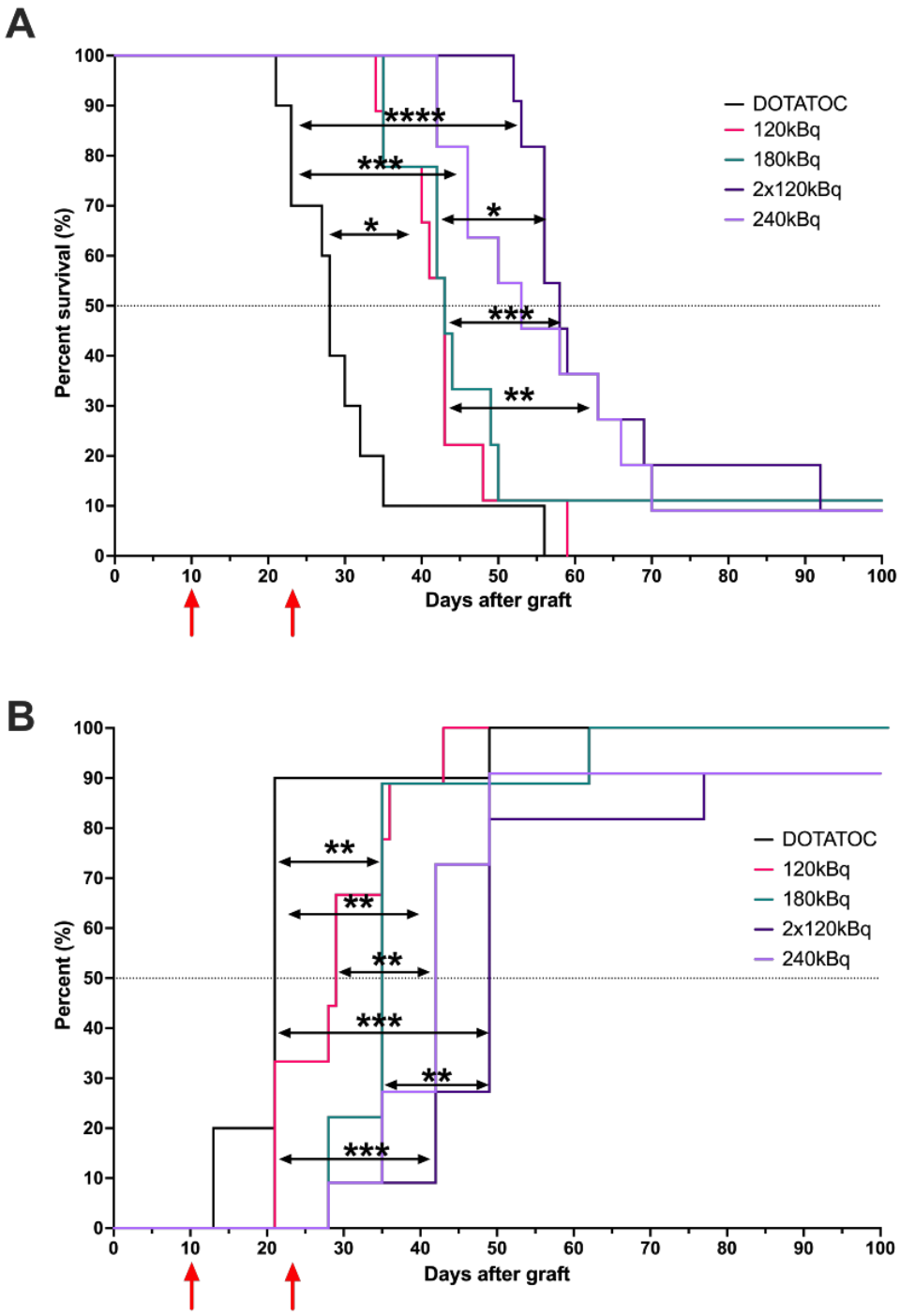

329

330

331

332

Toxicity of [^{225}Ac]Ac-DOTATOC in pancreatic neuroendocrine tumor liver micrometastases mice.

There was no significant loss in body weight after treatment in any of the groups. Weight loss never exceeded 10% in any group and by Day 23 after treatment (i.e. 33 days after graft), each mouse had recovered its initial weight or more (**Fig. 5, A).**

The complete blood count did not show a significant decrease in red blood cells or platelets after alpha-therapy. A transient and moderate decreased in white blood cells count after treatment, mainly due to a decrease in NK cells was observed. A drop in platelet counts over time related to disease progression was observed, as was seen rapidly in the DOTATOC group (**Fig. 5, B, C, D, E**).

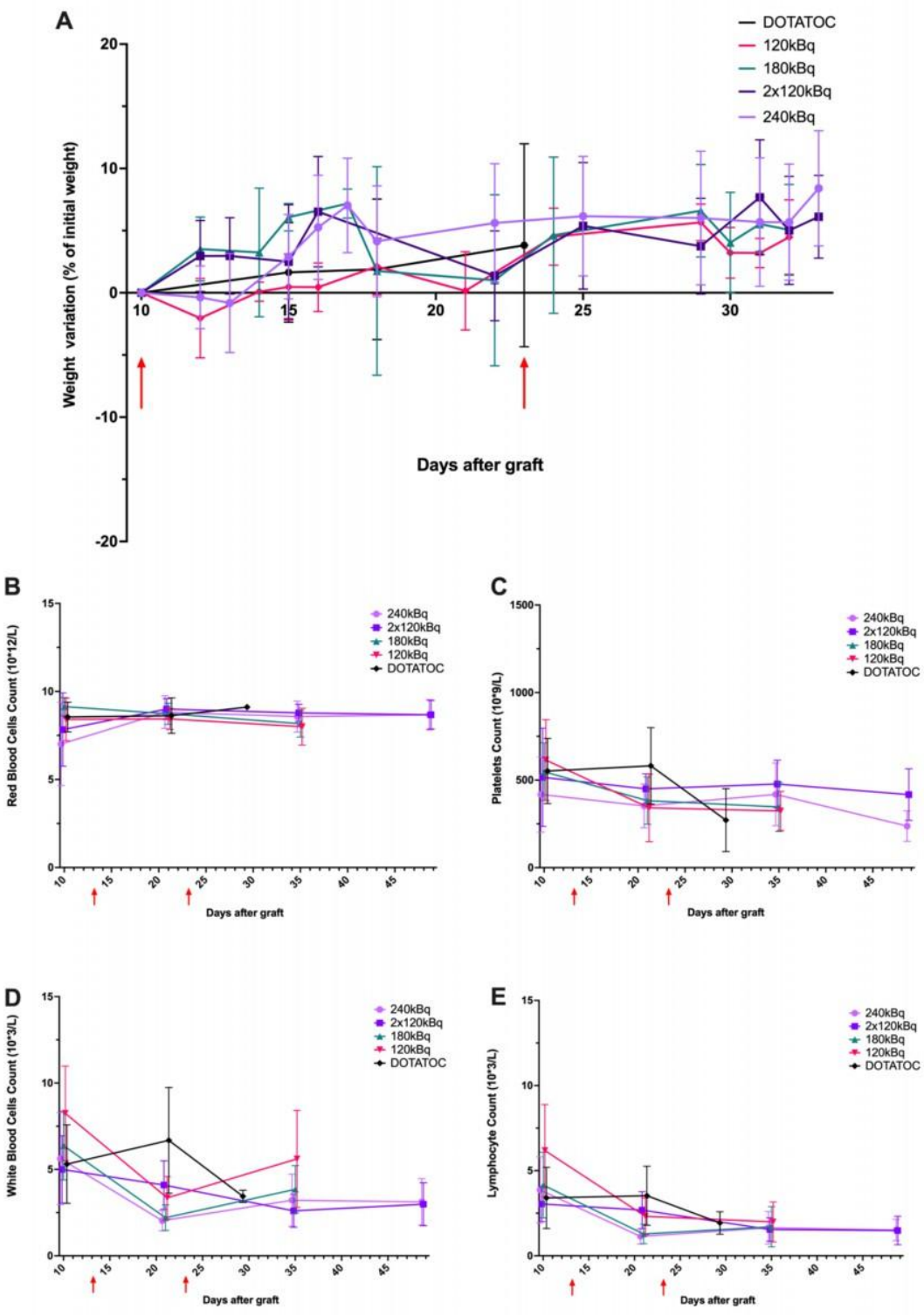
A
DOTATOC
120kBq
180kBq
2x120kBq
240kBq
Weight variation (% of initial weight)
Days after graft
B
Red Blood Cells Count (10*12/L)
C
Platelets Count (10*9/L)
D
White Blood Cells Count (10*3/L)
E
Lymphocyte Count (10*3/L)

342

343

344

To assess hepatic and renal toxicities we compared ALP, ALT, TBIL and BUN before engraftment and 10 days after alpha-therapy (D10). No acute hepatic or renal toxicity was observed at 10 days after treatment. At animal sacrifice (END), median ALT and TBIL values in all groups, including the DOTATOC group, were significantly higher than before tumor graft or at 10 days after treatment due to high tumoral liver burden leading to biliary obstruction with icterus and hepatic cytolysis whereas BUN was not significantly different. (**Fig. 6, A, B, C, D).**

Kidney anatomopathological analysis showed no severe lesions, with a semi-quantitative score of 3 or less per lesion. In each group, including the control group, one mouse had more lesions and a higher degree of damage than the others (mouse #3 in the DOTATOC group, mouse #13 in the 2x120 kBq group and mouse #23 in the 240 kBq group, **Supplemental Fig. 6**). There was no correlation between the number and the severity of histological lesions and the clinical condition of the animal at the time of sacrifice, neither with the creatinine and BUN. Details of lesions and their evaluation for each mouse and group are available in **Supplemental Table 3.**

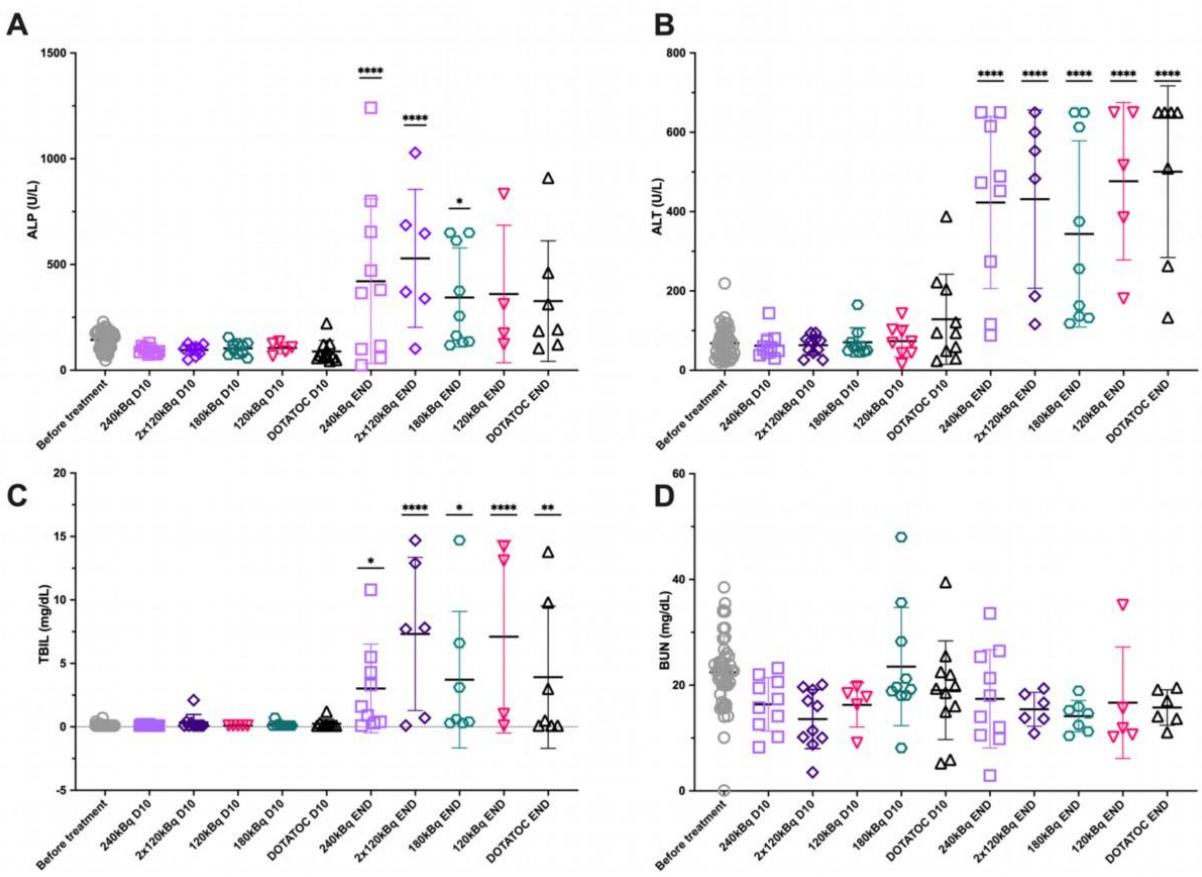

Fig. 6 *ALP (A), ALT (B), TBIL (C) and BUN (D) were assessed before graft, 10 days (D10) after alpha-therapy and at animal sacrifice (END). Statistical results shown are significantly different compared to "before treatment" point, (*) p < 0.03; (**) p < 0.002; (***) p < 0.0002; (****) p < 0.0001). ALP: alkaline phosphatase; ALT: alanine transaminase; BUN: blood urea nitrogen*

Discussion

Given the physical proprieties of alpha-particles, targeted alpha therapy seems a promising therapeutic approach for micrometastases, early relapse or minimal residual disease. Preclinical studies using SSA radiolabeled with ^{225}Ac have been previously performed using subcutaneous graft with macroscopic AR42J or H69 and H727 tumors [20,21]. In order to assess the efficacy and safety of a systemic treatment for GEP-NET, we aimed to propose a pertinent model of pancreatic NET liver micrometastases. Indeed, intraportal tumoral cells injection is an effective technique to rapidly induce liver metastases closely mirroring the pathophysiological progression observed in human disease and was previously performed in other preclinical cancers models [24,26]. In this study, we first demonstrated that it was possible to induce pNET liver metastases by intraportal injection and to study the development of the disease associated with an overall survival of 28 days. Splenic injection is another well-established method for inducing liver metastases. However, there are two potential drawbacks: either the spleen is not removed and the size of the tumor in the spleen may hinder imaging of liver metastases (especially for PET imaging due to a potential high uptake of the primary splenic tumor) or the spleen is removed in a second surgical procedure thereby increasing the risk of mortality for the animal [27–29]. Another less frequently encountered technique is orthotopic graft, particularly in the digestive tract and pancreas, followed by a wait for spontaneous development of liver metastasis. But it requires a large primary tumor mass that can lead to the death of the animal [30].

Secondly, we successfully performed a follow-up with MRI and phenotypic characterization with [^{68}Ga]Ga-DOTATOC and [^{18}F]F-FDG PET/MRI. This *in vivo* characterization allowed to confirm SSTR overexpression in a theranostic perspective before performing therapy studies. Indeed, SSTR expression in AR42J cells and tumors is known and has been previously studied [31–33] , but to our knowledge this is the first time that a comparison of [^{68}Ga]Ga-DOTATOC and [^{18}F]F-FDG by PET/MRI is carried out in a mouse model of NET liver metastases. Our results, showing high uptake of [^{68}Ga]Ga-DOTATOC but not [^{18}F]F-FDG, confirm that we have succeeded in producing a mouse model mimicking the well-differentiated phenotype encountered in the human disease with SSTR overexpression and relatively slow glucose metabolism.

One of the original aspects of this study is the treatment injection 10 days after intraportal tumor engraftment, before the development of macroscopic liver tumors. We aimed to study the specific context of residual disease after a first line treatment or adjuvant treatment to eradicate remaining cancer cells to avoid relapse. Given their characteristics which include the induction of double strand breaks and massive ionization, alpha particles are

more effective than other cytotoxic agents and can overcome resistance to chemotherapy or PRRT with beta-emitters [34,35].

In this model, [^{225}Ac]Ac-DOTATOC DLT was not reached. Dose escalation showed that a cumulated activity of 240 kBq was the most effective in improving survival. Three mice survived until Day 100. All mice developed tumors during follow-up except 2 in the groups treated with the highest activities (1 in 240kBq and 1 in 2x120kBq). One mouse in the 180kBq group developed tumors at Day 62 but managed to survive until the end of the experimentation. The fact that tumor-free mice were observed exclusively in the groups treated with the highest activities suggests that this occurrence is probably no mere coincidence but needs to be confirmed by further studies given the limited number of animals.

The therapeutic effect of [^{225}Ac]Ac-DOTATOC was associated with a moderate reduction in lymphocyte count, but no change in platelets or red blood cells. Some mice exhibited thrombopenia at the point of death, mainly due to the high tumor burden resulting in splenomegaly caused by intraportal hypertension. Similarly, we observed in all groups (including the DOTATOC one) an increase in TBIL, ALP and ALT at the point of death, caused by the high tumoral burden in the liver, leading to biliary obstruction and hepatic cytolysis. No liver toxicity was observed 10 days after treatment injection.

A previous preclinical study using [^{225}Ac]Ac-DOTATOC in mice bearing subcutaneous AR42J cell tumors showed that nephrotoxicity was the main limiting factor with radiation induced kidney tubular necrosis at activities greater than 30kBq [20]. In another study using [^{225}Ac]Ac-DOTATATE in mice bearing subcutaneous lung neuroendocrine cells tumors, no acute kidney damage was observed but chronic progressive nephropathy occurred in mice that received ≥111kBq. The renal toxicity of PRRT is well-known and studied. It is mainly explained by the fact that radiolabeled SSA are cleared via the kidneys and reabsorbed in the proximal tubular cells resulting in a high radiation dose to the kidneys [36]. The main way to overcome this risk of nephrotoxicity is the co-infusion with amino acids that blocks peptide tubular reabsorption [9,37]. However, in this study, we confirmed the favorable biodistribution of [^{225}Ac]Ac-DOTATOC with a rapid clearance from blood and a renal elimination but did not observe an increase in BUN with activities up to 240kBq during follow-up. Despite a significant initial renal accumulation of up to 22.84 ± 3.19% IA/g at 5 minutes, we did not observe renal toxicity as demonstrated by biochemical parameters and histological analysis. Our dosimetric study revealed, at the highest injected activity of 240 kBq, a mean absorbed dose of 12.1 ± 1.1 Gy to the kidneys. There are very few data on murine kidney toxicity following TAT treatments. Bäck et al. [38] showed that there was no significant

increase in BUN for kidney absorbed doses up to 15 Gy. Chan et al. estimated a kidney threshold absorbed dose of 11 Gy (at this absorbed dose, 5% of the animals died before 90 days) following a treatment with [^{213}Bi]Bi-DOTATATE in mice [39] . Our results are consistent with these previous findings. In external radiotherapy, the dose constraint to the kidneys is often estimated at 23 Gy, and initial PRRT studies were based on this constraint [40]. However, these data are difficult to extrapolate to this systemic treatment. The dose rate in PRRT is significantly lower than that in external irradiation and decreases over time due to the decay of the radiopharmaceutical [41]. Furthermore, other parameters must be considered, such as the biodistribution of the radiopharmaceutical in the kidneys and its residence time in this organ. Therefore, some authors prefer to use the biological effective dose (BED) to the kidneys, which considers the biological half-life of the radiopharmaceutical as well as the number of treatment cycles. This parameter is estimated at 40 Gy at the renal level in the context of PRRT [42]. In their study with [^{225}Ac]Ac-DOTATATE, Tafreshi *et al*. calculated a mean absorbed dose to the kidneys of 6.8 Gy/MBq and 5.9 Gy/MBq to the liver, significantly lower than our data [21]. However, our dosimetric analysis is based on biodistribution comprising 6 time points ranging from 5 minutes to 9 days compared to 3 time points (24h, 48h, and 96h) in that article. Therefore, with their model, they found a rapid decline in absorbed dose after the 96h time point, contrary to our data, explaining our dosimetry. Post-therapeutic single photon emission computed tomography/computed tomography (SPECT/CT) imaging could be an alternative method to achieve dosimetry, as demonstrated by Liubchenko et al. in prostate cancer patients treated with [^{225}Ac]Ac-PSMA-I&T [43]. However, it remains challenging to perform due to low therapeutic activities injected and the lack of well-established post-treatment imaging procedure, especially in pre-clinical models. Another approach to performing imaged-based dosimetry could be the use of ^{226}Ac SPECT imaging as a surrogate for ^{225}Ac prior to therapeutic injection [44].

These encouraging toxicity results suggest a potential clinical application of [^{225}Ac]Ac-DOTATOC in treating minimal residual disease. In such a scenario, where patients are potentially already cured, significant treatment-related side effects may not be justified.

To minimize damage to healthy tissue, cytotoxic treatments (including radiotherapy and chemotherapy) are usually delivered in fractions. For instance, PRRT with [^{177}Lu]Lu-DOTATATE is administered in 4-6 cycles every 6-12 weeks [45]. In this study, a group of mice was treated with 2 fractions of 120 kBq over a 13-day interval. The efficacy observed in this group, in terms of time to detection of the first tumor by MRI or overall survival was not significantly different from the group treated with a single injection of 240 kBq. However, it is interesting to note that both parameters were slightly and favorably delayed in the 2x120 kBq group, with no

additional toxicity observed. These results require further investigation, particularly with a more extended dose fractionation over time, which was not possible at the time of the study.

The first clinical experience using a SSA radiolabeled with ^{225}Ac was report by Ballal et al. in 32 patients with metastatic GEP-NETs who were progressive or stable after [^{177}Lu]Lu-DOTATATE PRRT [18]. Patients received 2 cycles of 100 kBq/kg of [^{225}Ac]Ac-DOTATATE by systemic injection with a two-month interval. The results reported that [^{225}Ac]Ac-DOTATATE could overcome [^{177}Lu]Lu-DOTATATE resistance with a disease control rate of 100% including 62.5% partial response and 37.5%. stable disease. The safety analysis revealed that no grade III/IV hematological, renal, or liver toxicities was observed but the median follow-up duration was only 8 months. The absence of severe toxicity was then confirmed in 2021 by a retrospective study which aimed to assess the maximum single cycle activity and cumulative activity which can be injected safely to patients. After a de-escalation study they showed that treatment activities of 20 MBq with 4 monthly repetitions and cumulative activity to 60-80 MBq were well tolerated [19]. These clinical studies already published and those ongoing using SSAs radiolabeled with 225Ac underscore several current challenges that remain largely unanswered. Questions persist regarding the optimal injected activity, the potential benefits of activity fractionation and dose repetition, the ideal therapeutic sequence, and the importance of nephroprotective treatment. Therefore, further preclinical studies are crucial to elucidate the underlying mechanisms and provide initial demonstrations.

Herein, we successfully demonstrate the efficacy in terms of tumor delay and survival, and the safety of [^{225}Ac]Ac-DOTATOC in a new relevant model of pancreatic NET liver metastases with MRI follow-up during experimentation. Since we did not reach a DLT in this model, further dose escalation and fractionation could be an improvement, as our data tend to show better efficacy with 2x120kBq. This mouse model could also be useful for assessing other potential treatments such as other radionuclide therapies targeting SSTR or the combination of PRRT and other cytotoxic agents.

Funding Declaration: this work has been supported in part by grants from the French National Agency for Research "France 2030 investment plan" Labex IRON (ANR-11-LABX-18-01) and RHU OPERANDI (ANR-21-RHUS-0012) and by grant from INCa-DGOS-INSERM/ITMO Cancer_18011 (SIRIC ILIAD) and by grant from “Fondation pour la Recherche Médicale” (FRM FDM202006011156).

Compliance with Ethical Standards

- **No potential conflicts of interest relevant to this article exist.**
- **Research involving animals**: all animal experiments were carried out in accordance with the European directive 2010/63/EU on the protection of laboratory animals and its transposition into French law (decree n 2013-118) and were conducted on the Experimental Therapeutic Unit platform (SFR François Bonamy, IRS-UN, University of Nantes, license number: D44-278).
- **Informed consent: not applicable**

Data Availability declaration: all data generated and analysed during this study are included in this published article and its supplementary information files.

Author Contribution declaration: the first draft of the manuscript was written by Alexandre Lugat. All cellular and animal experiments were carried out by Alexandre Lugat, Séverine Marionneau-Lambot, Mathilde Esnault and Sébastien Gouard. Data were interpreted by Alexandre Lugat, Françoise Kraeber-Bodéré, Catherine Ansquer and Joëlle Gaschet. Nicolas Chouin performed dosimetry studies; Florian Chocteau performed pathological analysis. Eric Frampas, Catherine Ansquer, Françoise Kraeber-Bodéré performed PET/MRI analysis. Alfred Morgenstern and Frank Bruchertseifer supplied the ^{225}Ac and contributed to the development of the radiolabeling process. Alexandre Lugat, Alain Faivre-Chauvet and Mickael Bourgeois performed radiolabeling with 68Ga and ^{225}Ac. Catherine Ansquer, Françoise Kraeber-Bodéré, Joëlle Gaschet designed the project and supervised all experimental procedures. All authors commented on previous versions of the manuscript. All authors critiqued to the manuscript and improved its intellectual content. All authors read and approved the final manuscript.

References

1. Dasari A, Shen C, Halperin D, Zhao B, Zhou S, Xu Y, et al. Trends in the Incidence, Prevalence, and Survival Outcomes in Patients With Neuroendocrine Tumors in the United States. JAMA Oncol. 2017;3:1335–42.
2. Reubi JC, Laissue J, Krenning E, Lamberts SW. Somatostatin receptors in human cancer: incidence, characteristics, functional correlates and clinical implications. J Steroid Biochem Mol Biol. 1992;43:27–35.
3. Volante M, Rosas R, Allìa E, Granata R, Baragli A, Muccioli G, et al. Somatostatin, cortistatin and their receptors in tumours. Mol Cell Endocrinol. 2008;286:219–29.
4. Krenning EP, Bakker WH, Breeman WA, Koper JW, Kooij PP, Ausema L, et al. Localisation of endocrine-related tumours with radioiodinated analogue of somatostatin. Lancet Lond Engl. 1989;1:242–4.
5. Scherübl H, Bäder M, Fett U, Hamm B, Schmidt-Gayk H, Koppenhagen K, et al. Somatostatin-receptor imaging of neuroendocrine gastroenteropancreatic tumors. Gastroenterology. 1993;105:1705–9.
6. Buchmann I, Henze M, Engelbrecht S, Eisenhut M, Runz A, Schäfer M, et al. Comparison of 68Ga-DOTATOC PET and 111In-DTPAOC (Octreoscan) SPECT in patients with neuroendocrine tumours. Eur J Nucl Med Mol Imaging. 2007;34:1617–26.
7. Hope TA, Pampaloni MH, Nakakura E, VanBrocklin H, Slater J, Jivan S, et al. Simultaneous 68Ga-DOTA-TOC PET/MRI with gadoxetate disodium in patients with neuroendocrine tumor. Abdom Imaging. 2015;40:1432–40.
8. Pavel M, Öberg K, Falconi M, Krenning EP, Sundin A, Perren A, et al. Gastroenteropancreatic neuroendocrine neoplasms: ESMO Clinical Practice Guidelines for diagnosis, treatment and follow-up†. Ann Oncol. 2020;31:844–60.
9. Strosberg J, El-Haddad G, Wolin E, Hendifar A, Yao J, Chasen B, et al. Phase 3 Trial of 177Lu-Dotatate for Midgut Neuroendocrine Tumors. N Engl J Med. 2017;376:125–35.
10. Bodei L, Cremonesi M, Grana CM, Fazio N, Iodice S, Baio SM, et al. Peptide receptor radionuclide therapy with 177Lu-DOTATATE: the IEO phase I-II study. Eur J Nucl Med Mol Imaging. 2011;38:2125–35.
11. Ballal S, Yadav MP, Damle NA, Sahoo RK, Bal C. Concomitant 177Lu-DOTATATE and Capecitabine Therapy in Patients With Advanced Neuroendocrine Tumors: A Long-term-Outcome, Toxicity, Survival, and Quality-of-Life Study. Clin Nucl Med. 2017;42:e457.
12. Bodei L, Kidd M, Paganelli G, Grana CM, Drozdov I, Cremonesi M, et al. Long-term tolerability of PRRT in 807 patients with neuroendocrine tumours: the value and limitations of clinical factors. Eur J Nucl Med Mol Imaging. 2015;42:5–19.
13. Strosberg JR, Caplin ME, Kunz PL, Ruszniewski PB, Bodei L, Hendifar A, et al. 177Lu-Dotatate plus long-acting octreotide versus high- dose long-acting octreotide in patients with midgut neuroendocrine tumours (NETTER-1): final overall survival and long-term safety results from an open-label, randomised, controlled, phase 3 trial. Lancet Oncol. 2021;22:1752–63.
14. Targeted Alpha Therapy Working Group, Parker C, Lewington V, Shore N, Kratochwil C, Levy M, et al. Targeted Alpha Therapy, an Emerging Class of Cancer Agents: A Review. JAMA Oncol. 2018;4:1765–72.
15. Cremonesi M, Ferrari M, Bodei L, Tosi G, Paganelli G. Dosimetry in Peptide Radionuclide Receptor Therapy: A Review. J Nucl Med. 2006;47:1467–75.
16. Makvandi M, Dupis E, Engle JW, Nortier FM, Fassbender ME, Simon S, et al. Alpha-Emitters and Targeted Alpha Therapy in Oncology: from Basic Science to Clinical Investigations. Target Oncol. 2018;13:189–203.
17. Eychenne R, Chérel M, Haddad F, Guérard F, Gestin J-F. Overview of the Most Promising Radionuclides for Targeted Alpha Therapy: The "Hopeful Eight." Pharmaceutics. 2021;13:906.
18. Ballal S, Yadav MP, Bal C, Sahoo RK, Tripathi M. Broadening horizons with 225Ac-DOTATATE targeted alpha therapy for gastroenteropancreatic neuroendocrine tumour patients stable or refractory to 177Lu-DOTATATE PRRT: first clinical experience on the efficacy and safety. Eur J Nucl Med Mol Imaging. 2019;
19. Kratochwil C, Apostolidis L, Rathke H, Apostolidis C, Bicu F, Bruchertseifer F, et al. Dosing 225Ac-DOTATOC in patients with somatostatin-receptor-positive solid tumors: 5-year follow-up of hematological and renal toxicity. Eur J Nucl Med Mol Imaging [Internet]. 2021 [cited 2021 Dec 21]; Available from: https://doi.org/10.1007/s00259-021-05474-1
20. Miederer M, Henriksen G, Alke A, Mossbrugger I, Quintanilla-Martinez L, Senekowitsch-Schmidtke R, et al. Preclinical Evaluation of the α-Particle Generator Nuclide 225Ac for Somatostatin Receptor Radiotherapy of Neuroendocrine Tumors. Clin Cancer Res. 2008;14:3555–61.
21. Tafreshi NK, Pandya DN, Tichacek CJ, Budzevich MM, Wang Z, Reff JN, et al. Preclinical evaluation of [225Ac]Ac-DOTA-TATE for treatment of lung neuroendocrine neoplasms. Eur J Nucl Med Mol Imaging [Internet]. 2021 [cited 2021 Aug 16]; Available from: http://link.springer.com/10.1007/s00259-021-05315-1
22. Pavel M, O''Toole D, Costa F, Capdevila J, Gross D, Kianmanesh R, et al. ENETS Consensus Guidelines Update for the Management of Distant Metastatic Disease of Intestinal, Pancreatic, Bronchial Neuroendocrine Neoplasms (NEN) and NEN of Unknown Primary Site. Neuroendocrinology. 2016;103:172–85.
23. Riihimäki M, Hemminki A, Sundquist K, Sundquist J, Hemminki K. The epidemiology of metastases in

neuroendocrine tumors. Int J Cancer. 2016;139:2679–86.
24. Frampas E, Maurel C, Thedrez P, Remaud-Le Saëc P, Faivre-Chauvet A, Barbet J. The intraportal injection model for liver metastasis: advantages of associated bioluminescence to assess tumor growth and influences on tumor uptake of radiolabeled anti-carcinoembryonic antigen antibody. Nucl Med Commun. 2011;32:147–54.
25. Frazier KS, Seely JC, Hard GC, Betton G, Burnett R, Nakatsuji S, et al. Proliferative and nonproliferative lesions of the rat and mouse urinary system. Toxicol Pathol. 2012;40:14S-86S.
26. Foubert F, Gouard S, Saï-Maurel C, Chérel M, Faivre-Chauvet A, Goldenberg DM, et al. Sensitivity of pretargeted immunoPET using 68Ga-peptide to detect colonic carcinoma liver metastases in a murine xenograft model: Comparison with 18FDG PET-CT. Oncotarget. 2018;9:27502–13.
27. Lavilla-Alonso S, Abo-Ramadan U, Halavaara J, Escutenaire S, Tatlisumak T, Saksela K, et al. Optimized Mouse Model for the Imaging of Tumor Metastasis upon Experimental Therapy. PLoS ONE [Internet]. 2011 [cited 2021 Apr 20];6. Available from: https://www.ncbi.nlm.nih.gov/pmc/articles/PMC3207818/
28. Pandit P, Johnston SM, Qi Y, Story J, Nelson R, Johnson GA. The utility of microCT and MRI in the assessment of longitudinal growth of liver metastases in a preclinical model of colon carcinoma. Acad Radiol. 2013;20:430–9.
29. Beuf O, Lartizien C, Milot L, Baboï L, Roche C, Langlois J-B, et al. Multimodal imaging for the detection and characterization of liver lesions in a mouse model of neuroendocrine tumor. Gastroentérologie Clin Biol. 2008;32:32–40.
30. Stelter L, Amthauer H, Rexin A, Pinkernelle J, Schulz P, Michel R, et al. An Orthotopic Model of Pancreatic Somatostatin Receptor (SSTR)-Positive Tumors Allows Bimodal Imaging Studies Using 3T MRI and Animal PET-Based Molecular Imaging of SSTR Expression. Neuroendocrinology. 2008;87:233–42.
31. Dam JH, Langkjær N, Baun C, Olsen BB, Nielsen AY, Thisgaard H. Preparation and Evaluation of [18F]AlF-NOTA-NOC for PET Imaging of Neuroendocrine Tumors: Comparison to [68Ga]Ga-DOTA/NOTA-NOC. Mol Basel Switz. 2022;27:6818.
32. Andersen TL, Baun C, Olsen BB, Dam JH, Thisgaard H. Improving Contrast and Detectability: Imaging with [55Co]Co-DOTATATE in Comparison with [64Cu]Cu-DOTATATE and [68Ga]Ga-DOTATATE. J Nucl Med Off Publ Soc Nucl Med. 2020;61:228–33.
33. Cal-Gonzalez J, Vaquero JJ, Herraiz JL, Pérez-Liva M, Soto-Montenegro ML, Peña-Zalbidea S, et al. Improving PET Quantification of Small Animal [68Ga]DOTA-Labeled PET/CT Studies by Using a CT-Based Positron Range Correction. Mol Imaging Biol [Internet]. 2018 [cited 2018 Mar 13]; Available from: http://link.springer.com/10.1007/s11307-018-1161-7
34. Mulford DA, Scheinberg DA, Jurcic JG. The Promise of Targeted α-Particle Therapy. J Nucl Med. 2005;46:199S-204S.
35. Kratochwil C, Bruchertseifer F, Rathke H, Hohenfellner M, Giesel FL, Haberkorn U, et al. Targeted α-Therapy of Metastatic Castration-Resistant Prostate Cancer with 225Ac-PSMA-617: Swimmer-Plot Analysis Suggests Efficacy Regarding Duration of Tumor Control. J Nucl Med Off Publ Soc Nucl Med. 2018;59:795–802.
36. Vegt E, de Jong M, Wetzels JFM, Masereeuw R, Melis M, Oyen WJG, et al. Renal toxicity of radiolabeled peptides and antibody fragments: mechanisms, impact on radionuclide therapy, and strategies for prevention. J Nucl Med Off Publ Soc Nucl Med. 2010;51:1049–58.
37. Rolleman EJ, Valkema R, de Jong M, Kooij PPM, Krenning EP. Safe and effective inhibition of renal uptake of radiolabelled octreotide by a combination of lysine and arginine. Eur J Nucl Med Mol Imaging. 2003;30:9–15.
38. Bäck T, Haraldsson B, Hultborn R, Jensen H, Johansson ME, Lindegren S, et al. Glomerular Filtration Rate After Alpha-Radioimmunotherapy with 211At-MX35-F(ab′)2: A Long-Term Study of Renal Function in Nude Mice. Cancer Biother Radiopharm. 2009;24:649–58.
39. Chan HS, Konijnenberg MW, Daniels T, Nysus M, Makvandi M, de Blois E, et al. Improved safety and efficacy of 213Bi-DOTATATE-targeted alpha therapy of somatostatin receptor-expressing neuroendocrine tumors in mice pre-treated with l-lysine. EJNMMI Res. 2016;6:83.
40. Emami B, Lyman J, Brown A, Cola L, Goitein M, Munzenrider JE, et al. Tolerance of normal tissue to therapeutic irradiation. Int J Radiat Oncol. 1991;21:109–22.
41. Menda Y, Madsen MT, O'Dorisio TM, Sunderland JJ, Watkins GL, Dillon JS, et al. 90Y-DOTATOC Dosimetry–Based Personalized Peptide Receptor Radionuclide Therapy. J Nucl Med. 2018;59:1692–8.
42. Bodei L, Cremonesi M, Ferrari M, Pacifici M, Grana CM, Bartolomei M, et al. Long-term evaluation of renal toxicity after peptide receptor radionuclide therapy with 90Y-DOTATOC and 177Lu-DOTATATE: the role of associated risk factors. Eur J Nucl Med Mol Imaging. 2008;35:1847–56.
43. Liubchenko G, Böning G, Zacherl M, Rumiantcev M, Unterrainer LM, Gildehaus FJ, et al. Image-based dosimetry for [225Ac]Ac-PSMA-I&T therapy and the effect of daughter-specific pharmacokinetics. Eur J Nucl Med Mol Imaging. 2024;51:2504–14.
44. Koniar H, Wharton L, Ingham A, Rodríguez-Rodríguez C, Kunz P, Radchenko V, et al. In vivoquantitative

SPECT imaging of actinium-226: feasibility and proof-of-concept. Phys Med Biol. 2024;69.
45. Zaknun JJ, Bodei L, Mueller-Brand J, Pavel ME, Baum RP, Hörsch D, et al. The joint IAEA, EANM, and SNMMI practical guidance on peptide receptor radionuclide therapy (PRRNT) in neuroendocrine tumours. Eur J Nucl Med Mol Imaging. 2013;40:800–16.